# BC8 Silicon (Si-III) is a Narrow-Gap Semiconductor

Haidong Zhang,[1,*] Hanyu Liu,[1] Kaya Wei,[2] Oleksandr O. Kurakevych,[3] Yann Le Godec,[3] Zhenxian Liu,[1] Joshua Martin,[4] Michael Guerrette,[1] George S. Nolas,[2] and Timothy A. Strobel[1,†]

[1]*Geophysical Laboratory, Carnegie Institution of Washington, Washington DC 20015, USA*

[2]*Department of Physics, University of South Florida, Tampa, Florida 33620, USA*

[3]*IMPMC, UPMC Sorbonne Universités, UMR CNRS 7590, Muséum National d'Histoire Naturelle, IRD UMR 206, F-75005 Paris, France*

[4]*Material Measurement Laboratory, National Institute of Standards and Technology, Gaithersburg, Maryland 20899, USA*

(Received 14 August 2016; revised manuscript received 4 January 2017; published 3 April 2017)

Large-volume, phase-pure synthesis of BC8 silicon ($Ia\bar{3}$, $cI16$) has enabled bulk measurements of optical, electronic, and thermal properties. Unlike previous reports that conclude BC8-Si is semimetallic, we demonstrate that this phase is a direct band gap semiconductor with a very small energy gap and moderate carrier concentration and mobility at room temperature, based on far- and midinfrared optical spectroscopy, temperature-dependent electrical conductivity, Seebeck and heat capacity measurements. Samples exhibit a plasma wavelength near 11 $\mu$m, indicating potential for infrared plasmonic applications. Thermal conductivity is reduced by 1–2 orders of magnitude depending on temperature as compared with the diamond cubic (DC-Si) phase. The electronic structure and dielectric properties can be reproduced by first-principles calculations with hybrid functionals after adjusting the level of exact Hartree–Fock (HF) exchange mixing. These results clarify existing limited and controversial experimental data sets and *ab initio* calculations.

DOI: 10.1103/PhysRevLett.118.146601

Silicon, probably the most important and widely used semiconductor, usually crystallizes in the diamond cubic structure (DC-Si, Si-I) with an indirect band gap of 1.1 eV. Aside from thermodynamically stable DC-Si, additional metastable allotropes can persist at ambient conditions: Si-III [1] (hereafter referred to as BC8, $Ia\bar{3}$, $cI16$), Si-IV [1] (hexagonal diamond, HD-Si, $P6_3/mmc$, $hP4$), Si-XII [2] ($R8$, $R\bar{3}$, $hR24$), zeolite types $Si_{136}$ [3] ($Fd\bar{3}m$, $cF136$), and $Si_{24}$ [4] ($Cmcm$, $oC24$) and several phases formed by laser-induced microexplosions [5]. Owing to fundamental differences in electronic structure between these "exotic" allotropes, many new properties and applications beyond those capable for DC-Si (e.g., direct band gap) could potentially be realized [6]. Unfortunately, only small quantities of these materials have been synthesized to date (often as impure mixed phases) preventing detailed characterization and fundamental understanding of intrinsic physical properties.

BC8-Si was first discovered in 1963 by Wentorf and Kasper [1]. The cubic structure contains one crystallographically unique silicon atom (Wyckoff position 16$c$ with atomic coordinate $x, x, x$) that is fourfold coordinated with one Si-Si distance at ~2.37 Å and the other three at ~2.38 Å in a distorted tetrahedral arrangement [1]. BC8-Si is usually obtained by compressing DC-Si to 11–14 GPa at room temperature to form metallic $\beta$-Sn-Si (Si-II) [7–11]. Decompression from Si-II follows a different structural sequence depending on the speed of pressure release. Slow decompression leads to the R8 phase between 10–2 GPa and further unloading to atmospheric pressure leads to BC8-Si, which persists at ambient pressure unless heated above ~200 °C [12,13]. While complete transformation of DC-Si to $\beta$-Sn-Si (and thereby BC8) requires pressures in excess of 10 GPa, recent studies indicate that chemical pathways involving sodium can reduce the formation pressure to as low as 7 GPa without the formation of $\beta$-Sn-Si [14]. In addition, an ambient-pressure colloidal synthesis route for BC8-Si nanoparticles was recently reported [15], which may serve useful for solar energy conversion applications with multiple exciton generation [16,17].

Theoretically, BC8-Si was first predicted to be a semiconductor with a direct band gap of 0.43 eV [18], and later calculated as a semimetal with either indirect [19] or direct [20,21] band overlap. Experimentally, many researchers have accessed this phase through diamond anvil cell (DAC) [2,22–26], nanoindentation [27–32] or shock experiments [33]. However, these techniques impose limitations on sample size (typically micron scale) and recovered samples often exist as mixed phases with DC-Si and/or R8 impurities. Consequently, a limited number of studies have reported properties characterization, aside from structure (density) and Raman scattering.

Besson *et al.* [34] measured the electrical conductivity of DAC-derived BC8-Si samples and suggested a micro-disordered, hole semimetal with conductivity between 50 to 333 S/cm at room temperature. Demishev *et al.* [35] examined the transition between BC8 and DC-Si and HD-Si, and measured an electrical conductivity of 290 S/cm for bulk samples obtained from a toroid-based

 © 2017 American Physical Society

apparatus. Wosylus *et al.* [36] measured electrical conductivity between 10 to 33 S/cm for bulk samples obtained from the multianvil technique. The reported conductivity values for BC8-Si are orders of magnitude more than typical semiconductors, for example, $3 \times 10^{-6}$ S/cm for undoped DC-Si [37], but several orders of magnitude less than typical metals, for example, $3.6 \times 10^{5}$ S/cm for Al [38]. Thus, primarily based on these results and recent *ab initio* calculations that include the *GW* approximation to the self-energy [21], BC8-Si is widely regarded to be a semimetal. It is noted, however, that the electrical conductivity of BC8-Si increased with temperature in previous measurements [34–36], behavior which is typically found in semiconductors. Furthermore, due to a lack of phase-pure bulk samples, there are presently no experimental reports on the optical or thermal transport properties for BC8-Si to the best of our knowledge.

In this work, we report optical and thermal measurements for BC8-Si as well as electrical transport and Seebeck characterization on phase-pure bulk samples. We find that BC8-Si is a semiconductor with an ultranarrow band gap of ~30 meV, and show that the thermal conductivity is 1–2 orders of magnitude lower than that of DC-Si. In addition, a plasma wavelength near 11 $\mu$m might serve useful for midinfrared-based plasmonics applications.

Bulk samples of BC8-Si were successfully synthesized via direct transformation of elemental silicon using the multianvil press method [39]. The recovered samples were characterized using x-ray diffraction, Raman spectroscopy, and nuclear magnetic resonance spectroscopy and were determined to be homogeneous, phase-pure specimens. Detailed characterization of samples can be found in Ref. [14]. An alternative set of phase-pure samples was obtained at 9.5 GPa in the Na-Si system [14]. These "chemical samples" were found to exhibit very similar physical properties, and are therefore not discussed separately.

Optical transmittance measurements on BC8-Si were performed in the far-IR regime in both $N_2$ and vacuum environments, as shown in Fig. 1(a). The data clearly show transmission increases below ~240 $cm^{-1}$, and the absorbance increases sharply above this value, indicating a fundamental band edge transition. Tauc plot [40] analysis, derived from this absorption feature shows linear dependence for $(\alpha l h\nu)^2$ versus $h\nu$ (where $\alpha$ is the absorption coefficient, $l$ is the samples thickness, and $h$ and $\nu$ are Planck's constant and frequency, respectively), indicating a direct band gap at $30 \pm 3$ meV, where the uncertainty is derived from a sensitivity analysis of the linear fit of the baseline and slope over different energy ranges. As the first optical characterization for BC8-Si in the far-IR region, this result is in contrast with the current assumption of the band overlap picture, and clearly indicates the existence of an ultranarrow gap.

To further probe the nature of the band gap, temperature-dependent, four-probe electrical conductivity measurements of BC8-Si were performed on bulk samples between 300 to 12 K. The temperature dependence of electrical resistivity for BC8-Si is shown in Fig. 1(b). The general trend is that the electrical resistivity decreased with temperature over the measurement range, indicating semiconducting behavior. This trend is consistent with the results from previous studies [34–36]. The conductivity of our BC8-Si is 76 S/cm at 300 K, compared to the values of 10–33 S/cm reported by Wosylus *et al.*, ~290 S/cm reported by Demishev *et al.*, and from 50–333 S/cm at 300 K reported by Besson *et al.* The results from all experiments are reasonably consistent, and differences in the magnitude of conductivity can likely be ascribed to differences in the phase transition efficiency (i.e., fraction of unconverted material) and in the starting material. The temperature dependence of the electrical conductivity for BC8-Si is similar to that of other narrow band gap semiconductors [41], InSb, for example, but exhibits a fundamentally different trend with either semimetals [42] (e.g., Bi, As, Sb) or metals [43] (e.g., Cu, Al). It is further noted that BC8-Si possesses a conductivity comparable to that of InSb (~230 S/cm at room temperature) [41], but 3–4 orders of magnitude smaller than those of typical semimetals [42], and 4–5 orders of magnitude smaller than those of typical metals [43].

When the thermal energy is sufficient to excite electrons across the band gap and to produce intrinsic charge carriers, the band gap of a semiconductor can be estimated by fitting the temperature dependence of the conductivity data as $\sigma(T) \approx \sigma_0 \exp[-(E_g/2k_BT)]$, where $\sigma(T)$ is the

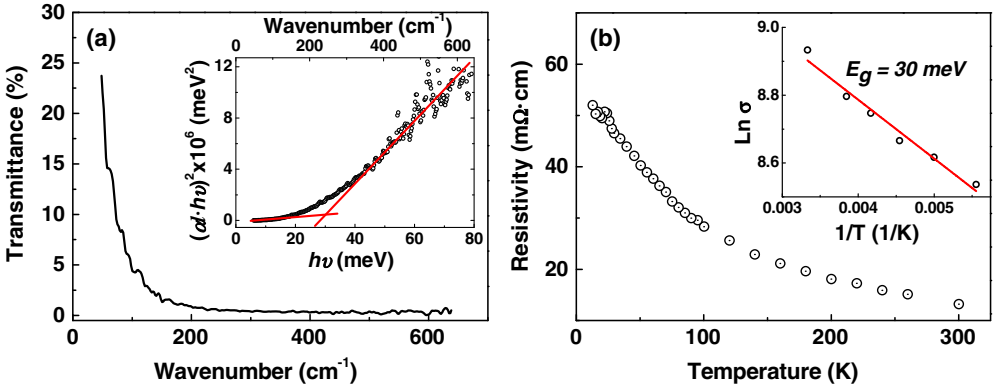


FIG. 1. (a) Optical transmittance spectrum for BC8-Si in the far-IR region. Tauc plot of the absorption, shown in the inset, reveals the fundamental direct band gap transition at ~30 meV. (b) Temperature dependence of the electrical resistivity for BC8-Si. Inset shows the activation energy fit to the data between 300 to 180 K.

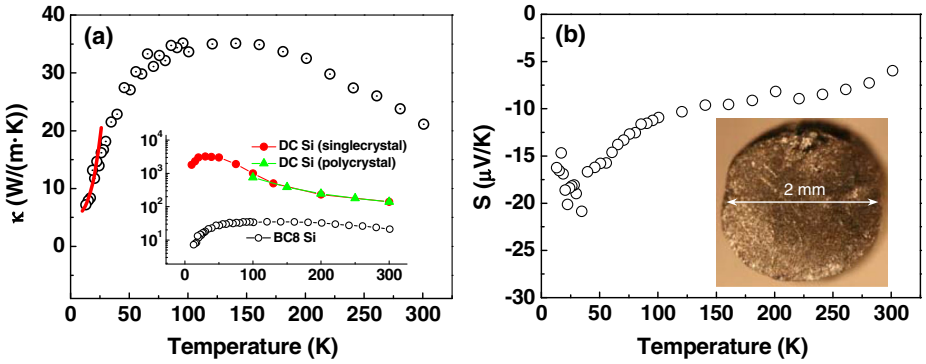


FIG. 2. (a) Temperature dependence of the thermal conductivity of BC8-Si. The solid line indicates a dependence of $T^3$ in the low-temperature regime. The inset shows a comparison of the thermal conductivity of BC8-Si with DC-Si [60,61] on a semi-log scale. (b) Temperature dependence of the Seebeck coefficient. The inset shows a picture of the sample with cylindrical shape.

temperature-dependent electrical conductivity, $\sigma_0$ is a material-related constant, $E_g$ is the band gap, $k_B$ is Boltzmann's constant, and $T$ is the temperature. By fitting an activation energy to our data between 300 and 180 K, we obtain a band gap of $30 \pm 8$ meV (where the uncertainty is from sensitivity analysis of the temperature range), in good agreement with the value obtained from the optical absorption measurements.

To further probe the optical response of BC8-Si, room-temperature optical reflectivity measurements were obtained in the midinfrared regime. Reflectivity spectra (see Supplemental Material [44], Fig. S1), exhibit a plasma edge near 900 $cm^{-1}$, indicative of mobile charge carriers. This behavior is not unexpected given the ultranarrow gap observed in the far IR and from the magnitude of electrical conductivity observed at room temperature. The band gap of 30 meV is close to the thermal energy corresponding to 293 K; hence, we expect to see conducting carriers at room temperature. Deeper insights into the interaction of the conduction band near-free electrons with incident light was obtained using a Drude-like relation (Supplemental Material [44]). This simple model is capable of reproducing the general features of the reflectivity spectra with a plasma wavelength $\lambda_p$ of 11.1 $\mu$m. The plasma wavelength is primarily determined by the density of mobile charge carriers in the medium, and, in this case, represents an interesting regime for potential plasmonic applications in the midinfrared that is difficult with conventional noble metal systems due to their large negative permittivities [59].

Using $m^* = 0.21m_0$ (derived from DFT calculations shown below), we estimate the carrier density of our BC8-Si samples to be $\sim 4.6 \times 10^{18}$ $cm^{-3}$ at room temperature. Conduction band mobile electrons are not only responsible for the optical response, but are also carriers for electrical conductivity. From the damping constant $\Gamma$ and electrical conductivity measurements, we also estimate the carrier density as $n = \Gamma m^* \sigma_0 / e^2 \approx 5.1 \times 10^{18}$ $cm^{-3}$, where $\sigma_0 = 76$ S/cm is the measured dc electrical conductivity, which is in good agreement with the value obtained from the optical measurements. From the measured conductivity, $\sigma = en\mu$, where $\sigma$, $e$, $n$, $\mu$ are electrical conductivity, electron charge, carrier density, and mobility, respectively, we further estimated the carrier mobility of BC8-Si to be $\sim 93$ $cm^2/(V \cdot s)$ at room temperature.

The thermal conductivity of BC8-Si, and its temperature dependence, was measured for the first time. As shown in Fig. 2(a), as temperature decreases, the thermal conductivity first increases from about 20–35 $W/(m \cdot K)$ between 300 to 125 K, then decreases to about 7 $W/(m \cdot K)$, while temperature drops to 12 K. Comparing with single-crystal [60] and polycrystalline [61] DC-Si, as shown in the inset of Fig. 2(a), the thermal conductivity of the well-sintered polycrystals of BC8-Si is 1–2 orders of magnitude lower depending on the exact temperature.

Also shown in Fig. 2(a), the thermal conductivity $\kappa$ is proportional to $T^3$ at low temperature, which is in agreement with the Debye $T^3$ law, suggesting a constant phonon mean free path with the thermal conductivity proportional to the heat capacity at low temperatures. Furthermore, the Lorenz number $L = \kappa/(\sigma \cdot T)$ for our sample is $9.3 \times 10^{-6}$ $W \cdot \Omega/K^2$ at 300 K. Comparing to a typical metal ($L_0 \approx 2.45 \times 10^{-8}$ $W \cdot \Omega/K^2$), the Lorenz number for BC8-Si is roughly 2 orders of magnitude higher, suggesting that the thermal conductivity comes mainly from the lattice contribution, not from the electron contribution normally seen in typical metals.

We further measured the Seebeck coefficient as a function of temperature. As shown in Fig. 2(b), the general trend is that the modulus of the Seebeck coefficient increases with temperature with a minimum at 25–30 K. The Seebeck coefficient for BC8-Si changes from $-6$ $\mu$V/K at 300 K to $-19$ $\mu$V/K at 20 K. Comparing to DC-Si, where the Seebeck coefficient for intrinsic DC-Si is $\sim -1.2$ mV/K (extrapolated value from high temperature) [61,62] for polycrystalline, and $\sim -440$ $\mu$V/K (extrapolated value from high temperature) for single crystal samples at 300 K [61], the Seebeck coefficient of BC8-Si is much smaller, which suggests a larger mobile carrier density, consistent with the large electrical conductivity and ultranarrow band gap feature. Additionally, the negative Seebeck coefficient suggests that electrons primarily dominate conduction, while the observed minimum could also suggest the importance of hole conduction at the lowest temperatures. We note that Demishev *et al.* [35] observed the Seebeck coefficient $\sim 2$ $\mu$V/K at 300 K,

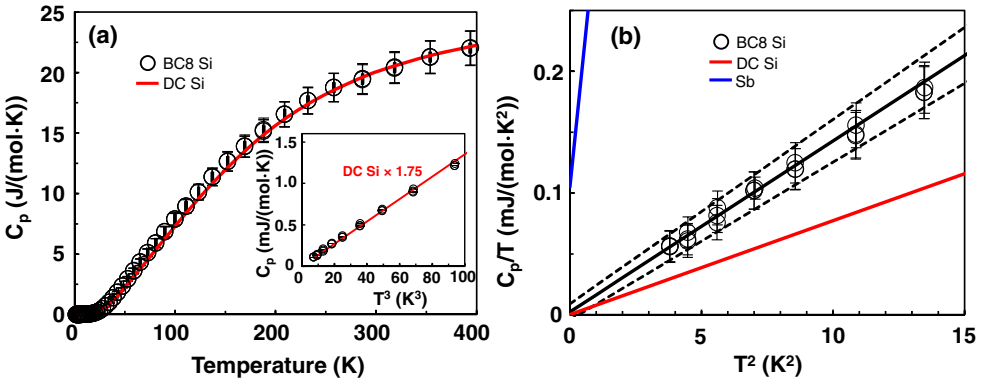


FIG. 3. (a) Temperature dependence of the heat capacity of BC8-Si compared with DC-Si [63]. The inset shows the low-temperature regime as a function of $T^3$ (DC-Si has been scaled by a factor of 1.75). (b) Heat capacity of BC8-Si plotted as $C/T$ versus $T^2$, compared with DC-Si (red line) and semimetallic antimony (blue line) [64]. The dashed lines indicate the 95% confidence interval for the BC8-Si linear regression.

suggesting $p$-type conductivity, and Besson *et al.* [34] observed hole conduction for their samples, which can be attributed to their use of $p$-type Si as a starting material.

Finally, we measured the temperature-dependent heat capacity $C_p$ between 2 and 400 K [Fig. 3(a)]. $C_p$ for BC8-Si is systematically greater than that of DC-Si, although their magnitudes are within our measurement error above 100 K. At temperatures well below the Debye temperature $\theta$, the heat capacity can be expressed as $C = \gamma T + AT^3$, where $\gamma$ and $A$ are materials constants related to electronic and phonon contributions, respectively. Figure 3(b) shows the low-temperature $C_p$ for BC8-Si plotted as $C_p/T$ versus $T^2$. Like DC-Si and other semiconducting materials, $C_p/T$ for BC8-Si tends towards zero as $T$ approaches 0 K. Linear regression of these data yield the equation $C_p/T = 0.002(3) + 0.0141(5)T^2$, where the electronic contribution to the heat capacity is statistically indistinguishable from zero and $\theta = 517(6)$ K. This behavior is fundamentally different from metals or semimetals [e.g., Sb in Fig. 3(b)], which exhibit finite values of $\gamma$ as $T \to 0$ K.

Given this new picture of the electronic structure of BC8-Si, it is of interest to investigate the influence of exchange-correlation energy with different functionals using density functional theory (DFT) to determine whether the narrow gap can be reproduced computationally. Like previous studies, we confirm that LDA and GGA (PBE) both result in small direct overlap at the $H$ point. After full relaxation within PBE, we obtain $a = 6.6569$ Å and $x = 0.1014$, in good agreement with our experimental values of $a = 6.62767(3)$ Å and $x = 0.10179(3)$ [14]. After applying the $GW$ correction to the PBE result, direct band overlap of ~0.15 eV still exists at the $H$ point, which is in agreement with previous theoretical calculations [21]. Similar to the study by Malone, Sau and Cohen [21], we also find that a band gap opens when the $x$ parameter is manually changed to a value of $x = 0.096$ [Fig. 4(b)]. Because the magnitude of band overlap is small and also sensitive to small changes in atomic coordinates, we decided to further investigate the impact of exchange correlation energy by calculating the band structure employing the HSE06 [65] hybrid functional, with different levels of exact Hartree-Fock (HF) exchange mixing. Using 25% HF mixing, it was still found that there is direct band overlap at the $H$ point as shown in Fig. 4(c). However, when the HF mixing fraction was increased to 35% a direct band gap of 10 meV was opened at the H point. For this case, the calculated unit cell parameters ($a = 6.6049$ Å, $x = 0.1008$) are still in good agreement with the experimental results and the narrow gap is reproduced without having to displace the atomic coordinates. While the level of HF mixing was adjusted to reproduce the experimental results, it would be of interest to examine the effectiveness of HF mixing to reproduce the electronic structures in other narrow-gap systems.

In contrast with the previous notion that BC8-Si is semimetallic, we show that this phase is actually an ultranarrow direct band gap semiconductor (~30 meV) from optical, electrical, and heat capacity measurements on our phase-pure bulk samples. This finding is reproduced

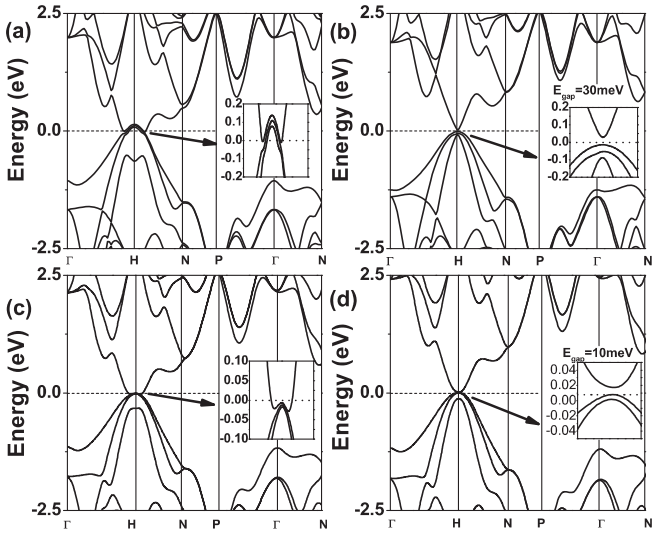


FIG. 4. The calculated bands structure with PBE + GW approximation (a) at $x = 0.101$ and (b) $x = 0.096$. (c) and (d) show the band structure calculations with the hybrid HSE functional using 25% and 35% exact HF exchange energy, respectively. The insets show the detailed band structure at the Fermi level.

by DFT calculations using hybrid pseudopotentials for the exchange-correlation energy, and may be useful to help guide future calculations on small-gap systems. Because of the narrow band gap, BC8-Si exhibits a plasma edge in the midinfrared and suggests potential for infrared plasmonic devices that could benefit a range of midinfrared applications [66]. Finally, we characterized the thermal properties of BC8-Si for the first time and demonstrate significantly reduced thermal conductivity and Seebeck coefficient compared with the DC-Si phase.

We are grateful to Dr. Y. Fei and Dr. W. Crichton for assistance with the *ex situ* and *in situ* multianvil experiments. We also thank Dr. C. Renero-Lecuna, Mr. K. Beneut, and Mr. M. Guillaumet for help in IR transmission and reflectance measurements on "chemical samples." This work was supported as part of the Energy Frontier Research in Extreme Environments (EFree) Center, an Energy Frontier Research Center funded by the U.S. Department of Energy, Office of Science under Award No. DE-SC0001057. Facilities and instrumentation support were provided by the following. Electrical and thermal properties characterization and analyses performed at USF were supported by the U.S. Department of Energy, Basic Energy Sciences, Division of Materials Science and Engineering, under Award No. DE-FG02-04ER46145. Infrared spectroscopy measurements performed at the National Synchrotron Light Source (NSLS II) were supported by National Science Foundation (EAR1606856, COMPRES) and DOE/NNSA (DE-NA-0002006, CDAC). Synthesis experiments in the Na-Si system with *in situ* XRD were performed at the ID06 beam line at the European Synchrotron Radiation Facility (ESRF), Grenoble, France, allocated to proposal CH-4109.

*haidongzhang@gmail.com
†tstrobel@carnegiescience.edu

[1] R. H. Wentorf Jr. and J. S. Kasper, Science **139**, 338 (1963).
[2] R. O. Piltz, J. R. Maclean, S. J. Clark, G. J. Ackland, P. D. Hatton, and J. Crain, Phys. Rev. B **52**, 4072 (1995).
[3] J. S. Kasper, P. Hagenmuller, M. Pouchard, and C. Cros, Science **150**, 1713 (1965).
[4] D. Y. Kim, S. Stefanoski, O. O. Kurakevych, and T. A. Strobel, Nat. Mater. **14**, 169 (2015).
[5] L. Rapp, B. Haberl, C. J. Pickard, J. E. Bradby, E. G. Gamaly, J. S. Williams, and A. V. Rode, Nat. Commun. **6**, 7555 (2015).
[6] B. Haberl, T. A. Strobel, and J. E. Bradby, Appl. Phys. Rev. **3**, 040808 (2016).
[7] J. C. Jamieson, Science **139**, 762 (1963).
[8] J. Z. Hu and I. L. Spain, Solid State Commun. **51**, 263 (1984).
[9] H. Olijnyk, S. K. Sikka, and W. B. Holzapfel, Phys. Lett. **103A**, 137 (1984).
[10] J. Z. Hu, L. D. Merkle, C. S. Menoni, and I. L. Spain, Phys. Rev. B **34**, 4679 (1986).
[11] M. I. McMahon, R. J. Nelmes, N. G. Wright, and D. R. Allan, Phys. Rev. B **50**, 739 (1994).
[12] J. Crain, G. J. Ackland, J. R. Maclean, R. O. Piltz, P. D. Hatton, and G. S. Pawley, Phys. Rev. B **50**, 13043(R) (1994).
[13] R. O. Piltz, J. R. Maclean, S. J. Clark, G. J. Ackland, P. D. Hatton, and J. Crain, Phys. Rev. B **52**, 4072 (1995).
[14] O. O. Kurakevych, Y. L. Godec, W. A. Crichton, J. Guignard, T. A. Strobel, H. Zhang, H. Liu, C. C. Diogo, A. Polian, N. Menguy *et al.* Inorg. Chem. **55**, 8943 (2016).
[15] S. Ganguly, N. Kazem, D. Carter, and S. M. Kauzlarich, J. Am. Chem. Soc. **136**, 1296 (2014).
[16] S. Wippermann, M. Vörös, D. Rocca, A. Gali, G. Zimanyi, and G. Galli, Phys. Rev. Lett. **110**, 046804 (2013).
[17] T. Arguirov, T. Mchedlidze, M. Kittler, R. Rölver, B. Berghoff, M. Först, and B. Spangenberg, Appl. Phys. Lett. **89**, 053111 (2006).
[18] J. D. Joannopoulos and M. L. Cohen, Phys. Rev. B **7**, 2644 (1973).
[19] R. Biswas, R. M. Martin, R. J. Needs, and O. H. Nielsen, Phys. Rev. B **35**, 9559 (1987).
[20] B. G. Pfrommer, M. Côté, S. G. Louie, and M. L. Cohen, Phys. Rev. B **56**, 6662 (1997).
[21] B. D. Malone, J. D. Sau, and M. L. Cohen, Phys. Rev. B **78**, 035210 (2008).
[22] H. Olijnyk, S. K. Sikka, and W. B. Holzapfel, Phys. Lett. **103A**, 137 (1984).
[23] G. Weill, J. L. Mansot, G. Sagon, C. Carlone, and J. M. Besson, Semicond. Sci. Technol. **4**, 280 (1989).
[24] M. I. McMahon and R. J. Nelmes, Phys. Rev. B **47**, 8337 (1993).
[25] M. Hanfland, U. Schwarz, K. Syassen, and K. Takemura, Phys. Rev. Lett. **82**, 1197 (1999).
[26] B. Haberl, M. Guthrie, S. V. Sinogeikin, G. Shen, J. S. Williams, and J. E. Bradby, High Press. Res. **35**, 99 (2015).
[27] A. P. Gerk and D. Tabor, Nature (London) **271**, 732 (1978).
[28] D. R. Clarke, M. C. Kroll, P. D. Kirchner, R. F. Cook, and B. J. Hockey, Phys. Rev. Lett. **60**, 2156 (1988).
[29] A. Kailer, K. G. Nickel, and Y. G. Gogotsi, J. Raman Spectrosc. **30**, 939 (1999).
[30] J. E. Bradby, J. S. Williams, and M. V. Swain, Phys. Rev. B **67**, 085205 (2003).
[31] D. Ge, V. Domnich, and Y. Gogotsi, J. Appl. Phys. **95**, 2725 (2004).
[32] S. Ruffell, B. Haberl, S. Koenig, J. E. Bradby, and J. S. Williams, J. Appl. Phys. **105**, 093513 (2009).
[33] M. J. Smith, Y.-T. Lin, M.-J. Sher, M. T. Winkler, E. Mazur, and S. Gradečak, J. Appl. Phys. **110**, 053524 (2011).
[34] J. M. Besson, E. H. Mokhtari, J. Gonzalez, and G. Weill, Phys. Rev. Lett. **59**, 473 (1987).
[35] S. V. Demishev, D. G. Lunts, D. V. Nekhaev, N. E. Sluchanko, N. A. Samarin, V. V. Brazhkin, A. G. Lyapin, S. V. Popova, and N. N. Mel'nik, ZhETF **109**, 2150 (1996) [, J. Exp. Theor. Phys. **82**, 1159 (1996)].
[36] A. Wosylus, H. Rosner, W. Schnelle, and U. Schwarz, Z. Anorg. Allg. Chem. **635**, 700 (2009).
[37] S. M. Sze, *Semiconductor Devices, Physics and Technology,* 2nd ed. (John Wiley & Sons, New York, 2002), p. 538.
[38] R. A. Serway, *Principles of Physics,* 2nd ed. (Saunders College Pub., Fort Worth, Texas; London, 1998), p. 602.

[39] C. M. Bertka and Y. Fei, J. Geophys. Res. **102**, 5251 (1997).
[40] J. Tauc, R. Grigorovici, and A. Vancu, Phys. Status Solidi **15**, 627 (1966).
[41] H. J. Hrostowski, F. J. Morin, T. H. Geballe, and G. H. Wheatley, Phys. Rev. **100**, 1672 (1955).
[42] J-P. Issi, Aust. J. Phys. **32**, 585 (1979).
[43] G. W. C. Kaye and T. H. Laby, *Tables of Physical and Chemical Constants* (Longmans Green, London, 1966).
[44] See Supplemental Material at http://link.aps.org/supplemental/10.1103/PhysRevLett.118.146601 for detailed information on sample synthesis, properties characterization, computational method, and optical reflectivity analysis, which includes Refs. [45–58].
[45] Certain commercial equipment, instrumentation, or materials are identified in this document. Such identification does not imply recommendation or endorsement by the National Institute of Standards and Technology, nor does it imply that the products identified are necessarily the best available for the purpose.
[46] J. Martin, G. S. Nolas, H. Wang, and J. Yang, J. Appl. Phys. **99**, 044903 (2006).
[47] J. Martin and G. S. Nolas, Rev. Sci. Instrum. **87**, 015105 (2016).
[48] J. P. Perdew, K. Burke, and M. Ernzerhof, Phys. Rev. Lett. **77**, 3865 (1996).
[49] G. Kresse and J. Hafner, Phys. Rev. B **49**, 14251 (1994).
[50] G. Kresse and J. Furthmüller, Phys. Rev. B **54**, 11169 (1996).
[51] G. Kresse and J. Hafner, Phys. Rev. B **47**, 558(R) (1993).
[52] P. E. Blöchl, Phys. Rev. B **50**, 17953 (1994).
[53] G. Kresse and D. Joubert, Phys. Rev. B **59**, 1758 (1999).
[54] A. A. Mostofi, J. R. Yates, Y.-S. Lee, I. Souza, D. Vanderbilt, and N. Marzari, Comput. Phys. Commun. **178**, 685 (2008).
[55] N. Marzari and D. Vanderbilt, Phys. Rev. B **56**, 12847 (1997).
[56] I. Souza, N. Marzari, and D. Vanderbilt, Phys. Rev. B **65**, 035109 (2001).
[57] A. A. Mostofi, J. R. Yates, G. Pizzi, Y.-S. Lee, I. Souza, D. Vanderbilt, and N. Marzari, Comput. Phys. Commun. **185**, 2309 (2014).
[58] J. Heyd, G. E. Scuseria, and M. Ernzerhof, J. Chem. Phys. **124**, 219906 (2006).
[59] S. Law, V. Podolskiy, and D. Wasserman, Nanophotonics **2**, 103 (2013).
[60] C. J. Glassbrenner and G. A. Slack, Phys. Rev. **134**, A1058 (1964).
[61] W. Fulkerson, J. P. Moore, R. K. Williams, R. S. Graves, and D. L. McElroy, Phys. Rev. **167**, 765 (1968).
[62] T. Geballe and G. Hull, Phys. Rev. **98**, 940 (1955).
[63] P. D. Desai, J. Phys. Chem. Ref. Data **15**, 967 (1986).
[64] D. C. McCollum and W. A. Taylor, Phys. Rev. **156**, 782 (1967).
[65] A. A. Mostofi, J. R. Yates, Y.-S. Lee, I. Souza, D. Vanderbilt, and N. Marzari, Comput. Phys. Commun. **178**, 685 (2008).
[66] S. Law, R. Liu, and D. Wasserman, J. Vac. Sci. Technol. B **32**, 052601 (2014).